

Supplementary Materials for

A potent CBP/p300-Snail interaction inhibitor suppresses tumor growth and metastasis in wild-type p53-expressing cancer

Hong-Mei Li, Yan-Ran Bi, Yang Li, Rong Fu, Wen-Cong Lv, Nan Jiang, Ying Xu, Bo-Xue Ren, Ya-Dong Chen, Hui Xie, Shui Wang, Tao Lu*, Zhao-Qiu Wu*

*Corresponding author. Email: zqwu@cpu.edu.cn (Z.-Q.W.); lutao@cpu.edu.cn (T.L.)

Published 22 April 2020, *Sci. Adv.* **6**, eaaw8500 (2020)
DOI: 10.1126/sciadv.aaw8500

This PDF file includes:

Figs. S1 to S7

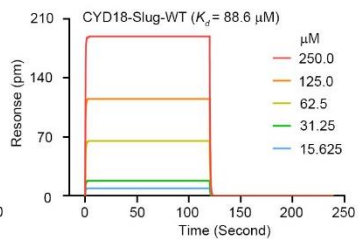
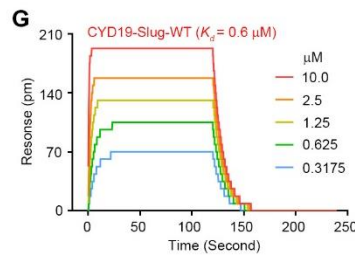
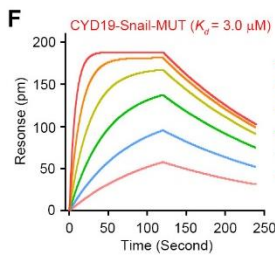
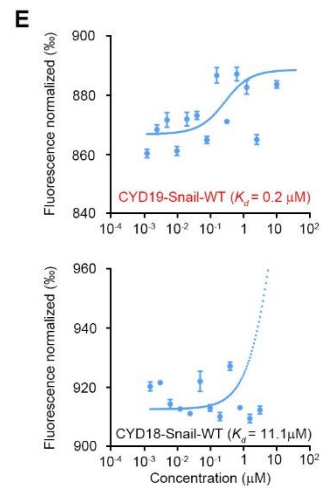
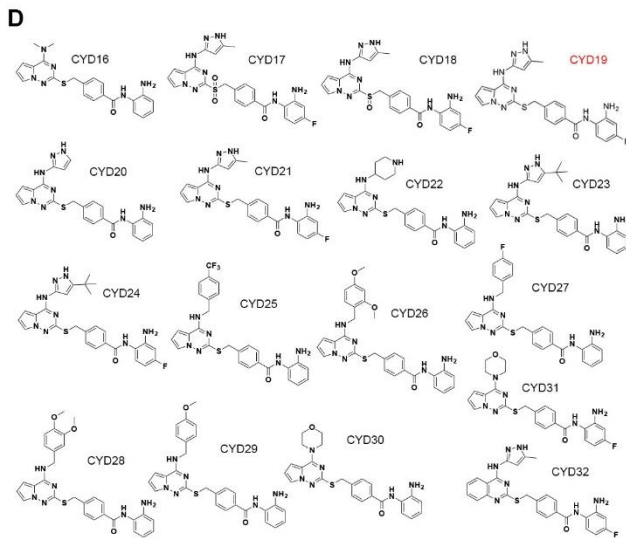
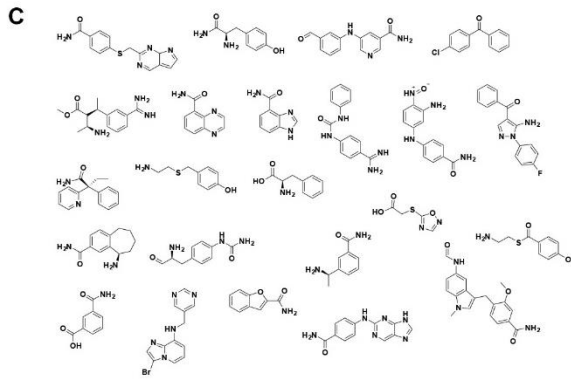
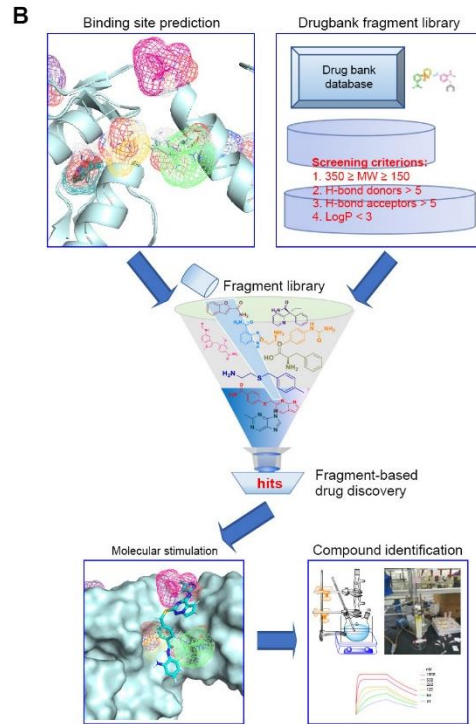
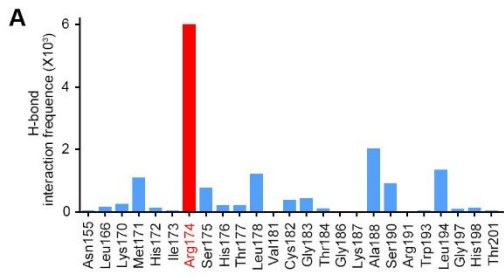


Fig. S1. Screening of the small-molecule compound CYD19 that forms a high-affinity interaction with Snail protein. (A) Identification of R174 pocket as a key “hot spot”. The profile of mapping fingerprint, which is generated by calculating a percentage contact frequency for each amino acid, consists of the amino acids with the highest percentage of contact frequencies. The contact frequency for an individual amino acid (aa_i) was calculated using the formula: number of H-bonded contacts for aa_i / sum of contacts for all aa. (B) Workflow of the screening and rational design of small-molecule compounds forming potential interaction with Snail protein. (C) Chemical structures of fragments from DrugBank database based on the specific screening condition. (D) Chemical structures of small-molecule compounds forming potential interaction with Snail protein. (E) MST analysis to measure dissociation kinetics of compounds towards Snail-WT recombinant proteins. (F and G) BLI analysis to measure dissociation kinetics of compounds towards Snail-R174A (F) or Slug-WT (G) recombinant protein.

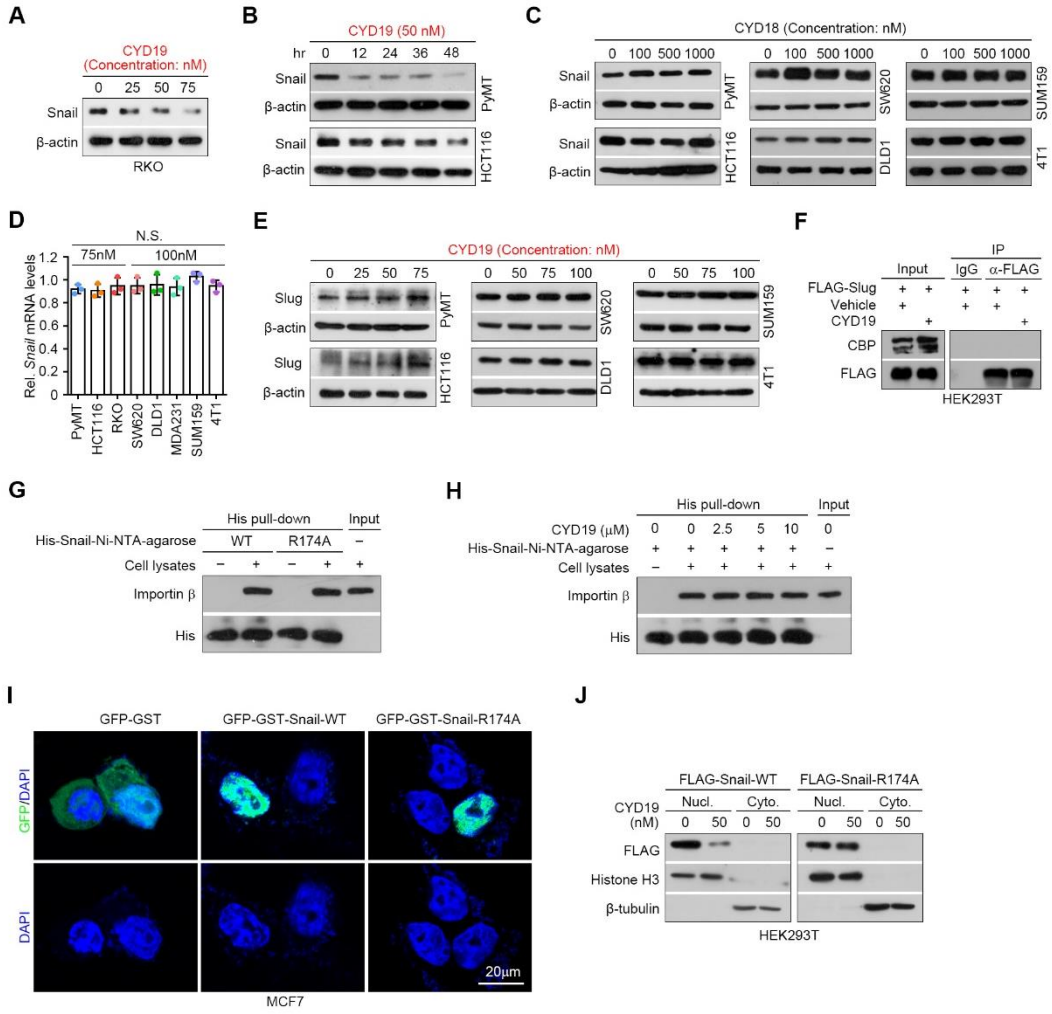


Fig. S2. CYD19 suppresses Snail expression but does not impact its subcellular localization. (A) Immunoblot analysis of Snail expression in RKO cells treated with vehicle or CYD19 for 48 h. (B) Immunoblot analysis of Snail expression in PyMT and HCT116 cells treated with vehicle or 50 nM CYD19 for different times. (C) Immunoblot analysis of Snail expression in cancer cells treated with vehicle or CYD19 for 48 h. (D) RT-qPCR analysis of *Snail* expression in cancer cells treated with vehicle or CYD19 for 48 h. (E) Immunoblot analysis of Slug expression in cancer cells treated with vehicle or CYD19 for 48 h. (F) Binding interaction of exogenous Slug with endogenous CBP was monitored in cells that were treated with vehicle or 50 nM CYD19 for 48 h. (G) His pull-down assay to assess association of His-Snail-WT or -R174A with exogenous importin β . (H) His pull-down assay to assess CYD19's impact on association of His-Snail-WT with exogenous importin β in the presence of vehicle or CYD19. (I) Immunofluorescence analysis for GFP-GST-, GFP-GST-Snail-WT- or GFP-GST-Snail-R174A- transfected MCF7 cells. (J) Immunoblot analysis of exogenous Snail-WT and Snail-R174A expressions in nuclear and cytoplasmic compartments of cancer cells that were treated with vehicle or 50 nM CYD19 for 48 h. Histone-H3 and β -tubulin are used as nuclear and cytoplasmic markers, respectively. All representative blots as shown are from three independent experiments. Data are presented as mean \pm S.D. (n = 3 independent experiments). N.S., not significant. Differences are tested using unpaired two-sided Student's t-test.

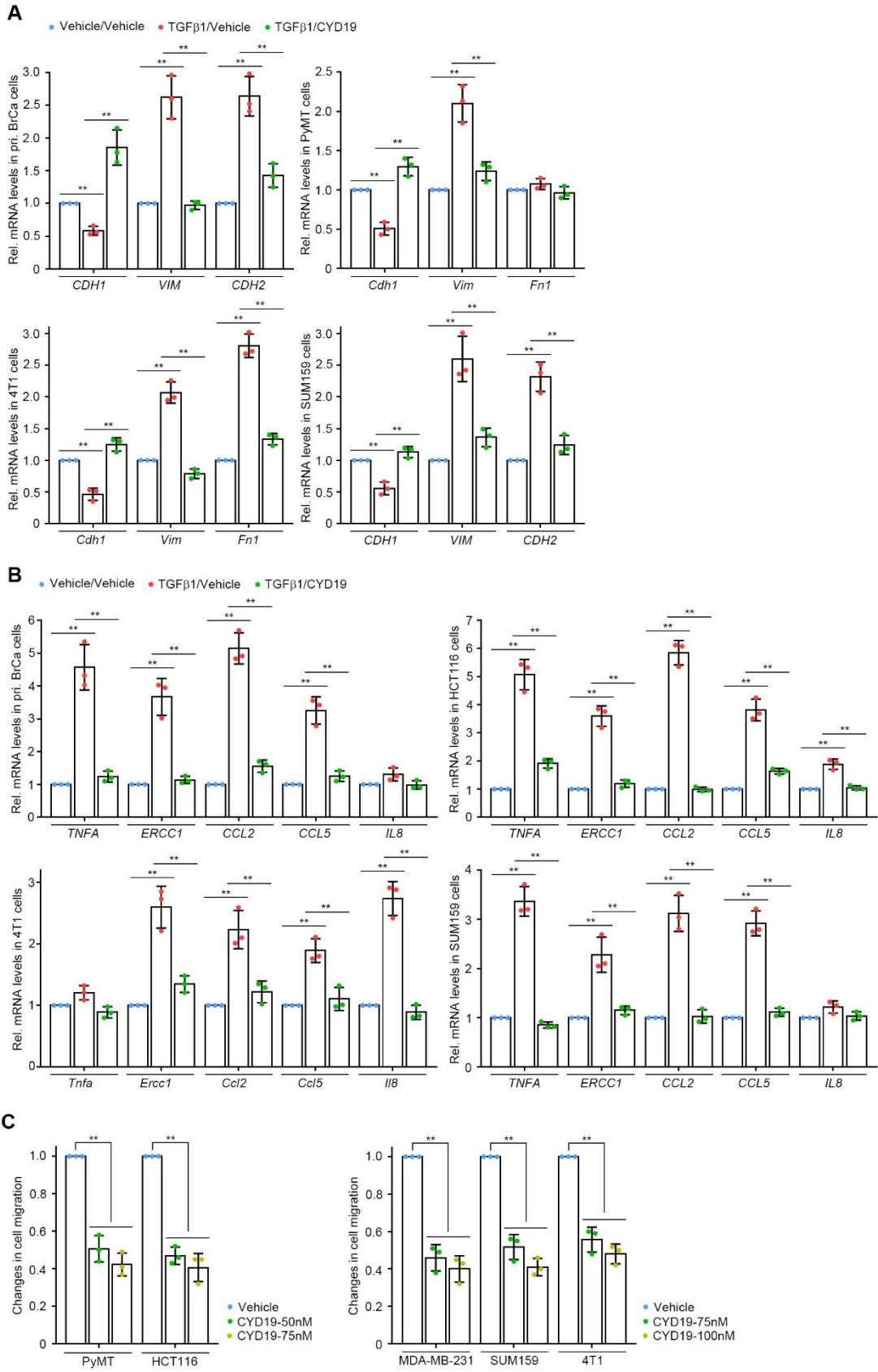


Fig. S3. CYD19 inhibits Snail-driven EMT and migration in cancer cells. (A) RT-qPCR analysis of *Cdh1*, *Vim*, *Fn1* and *Cdh2* expressions in primary cells and cell lines that were treated with vehicle or 2 ng/ml TGF β 1 for 24 h and then with vehicle or CYD19 in the presence of TGF β 1 for another 48 h. (B) RT-qPCR analysis of *TNF α* , *ERCC1*, *CCL2*, *CCL5* and *IL8* expressions in cells as described in A. (C) Equal numbers (2×10^5 cells per well) of cancer cells pretreated with vehicle or CYD19 for 48 h were subjected to cell migration assays, and invaded cells were quantified. All data are presented as mean \pm S.D. (n = 3 independent experiments). ** $P < 0.01$. Differences are tested using one-way ANOVA with Tukey's post hoc test.

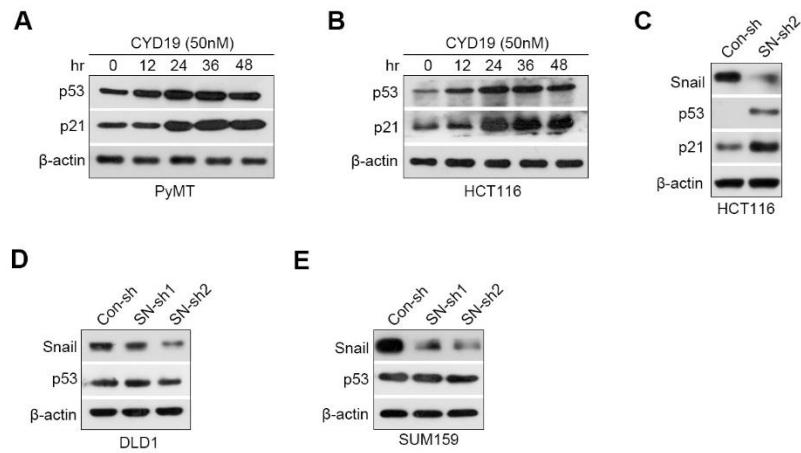


Fig. S4. CYD19 reverses Snail-dependent repression of wild-type p53. (A and B) Immunoblot analysis of p53 and p21 expressions in PyMT (A) and HCT116 (B) cells that were treated with vehicle or CYD19 for different times. (C) Immunoblot analysis of Snail, p53 and p21 expressions in control and p53-silenced PyMT cells. (D and E) Immunoblot analysis of Snail and p53 expressions in control and p53-silenced DLD1 (D) and SUM159 (E) cells. All representative blots as shown are from three independent experiments.

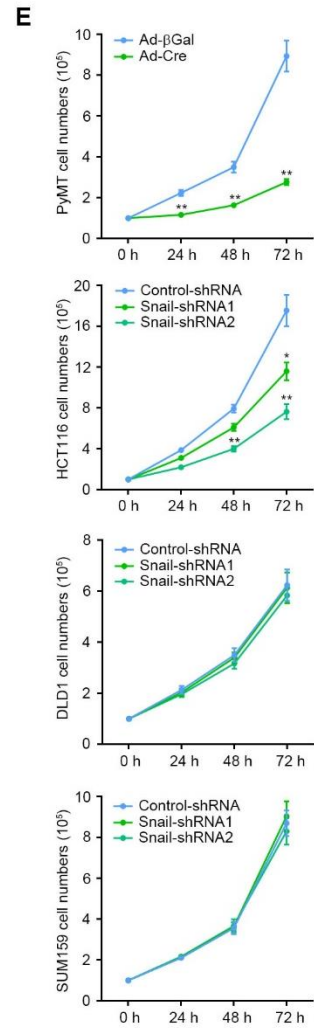
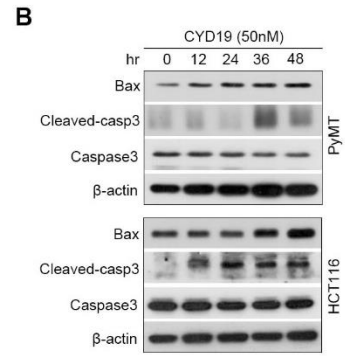
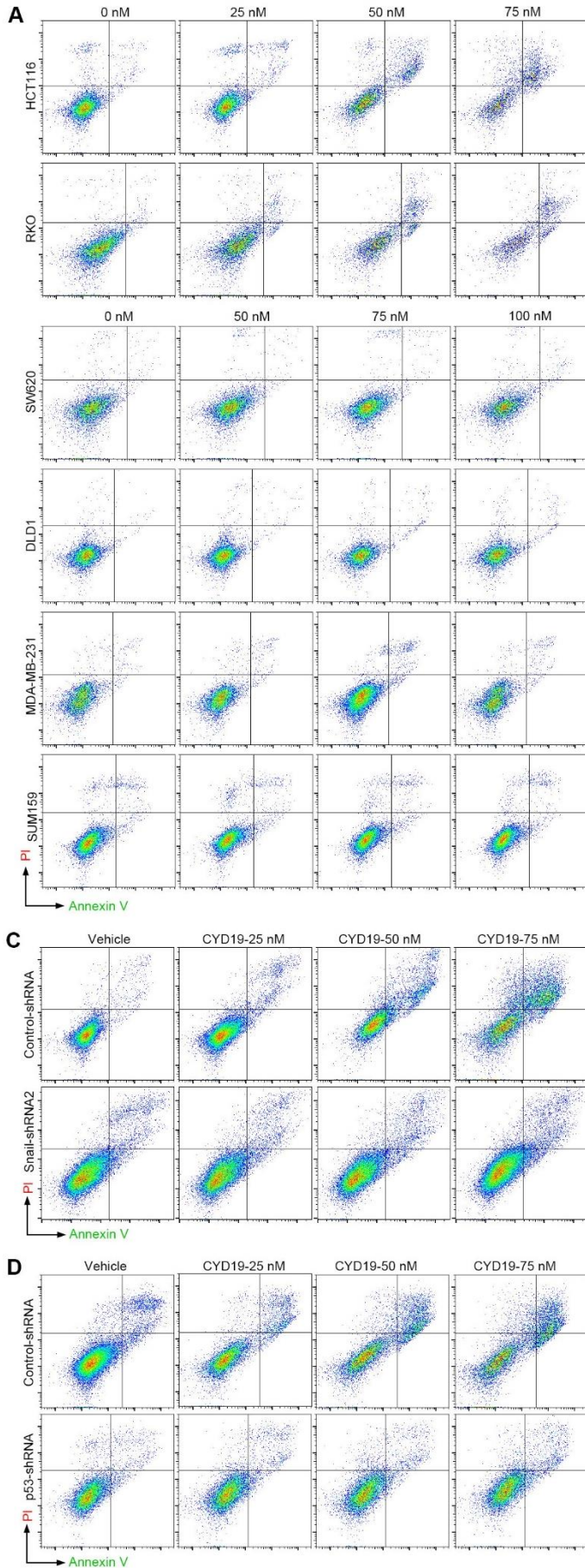


Fig. S5. CYD19 suppresses proliferation and survival of cancer cells expressing wild-type p53. (A) Representative histogram of apoptotic subpopulation in various cell lines that were treated with vehicle or CYD19 for 48 h. (B) Immunoblot analysis of the indicated protein expressions in cells that were treated with vehicle or CYD19 for different times. (C and D) Representative histogram of apoptotic subpopulation in control and Snail-silenced (C) or p53-silenced (D) HCT116 cells treated with vehicle or CYD19 for 48 h. (E) CCK-8 assays for control and Snail-silenced cells treated with vehicle or CYD19 for 48 h. All representative blots and histograms as shown are from three independent experiments. All data are presented as mean \pm S.D. (n = 3 independent experiments). ** $P < 0.01$. Differences are tested using one-way ANOVA with Tukey's post hoc test.

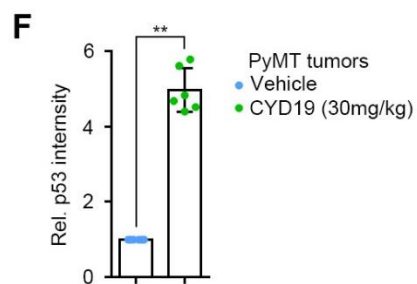
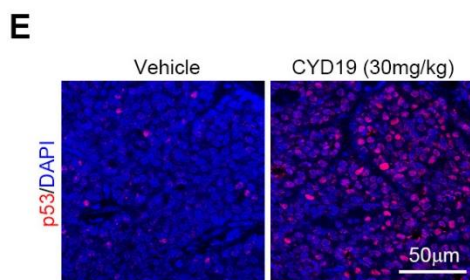
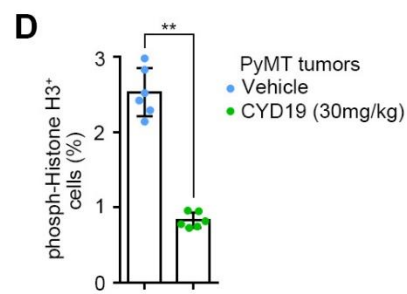
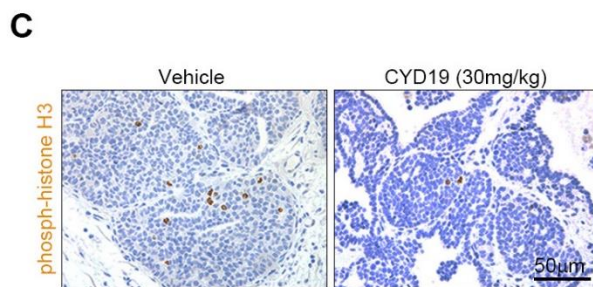
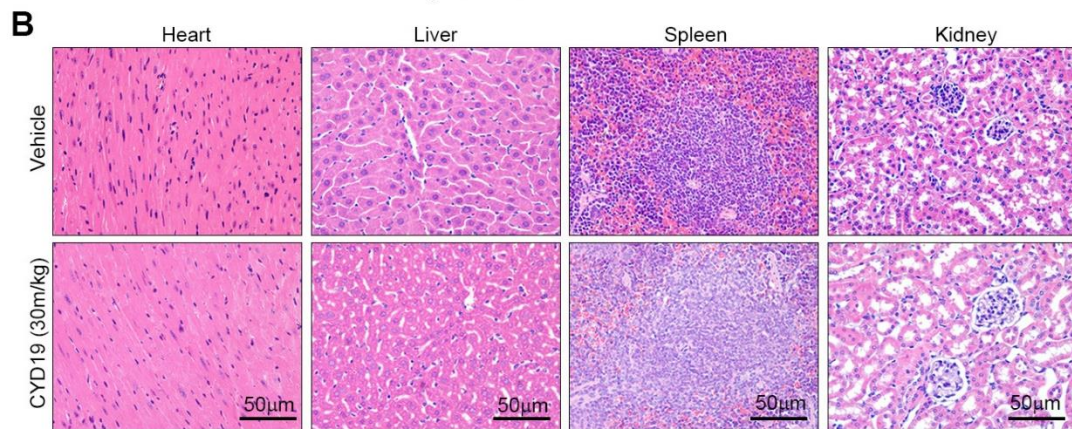
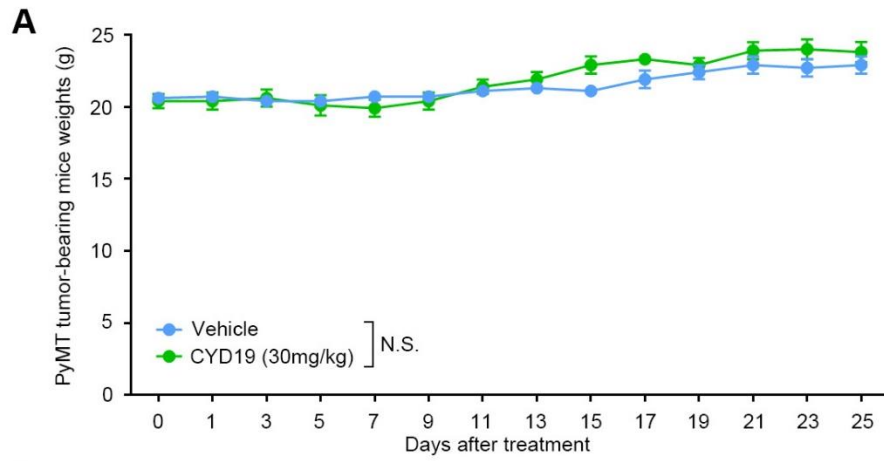


Fig. S6. CYD19 suppresses Snail-driven PyMT tumor progression without eliciting toxicity on tumor-bearing mice. (A) Body weights of MMTV-PyMT mice that were intraperitoneally treated with vehicle or CYD19 for 25 consecutive days (n = 6 mice, each). (B) Representative H&E images of heart, liver, spleen and kidney of tumor-bearing mice as described in A. (C) Immunohistochemical staining of phospho-histone H3 in primary tumors of vehicle- and CYD19-treated mice (n = 6 mice, each). (D) Quantification of phospho-histone H3-positive cells in primary tumors as described in C. (E) Immunofluorescence staining of p53 in tumors as described in C. (F) Quantification of staining intensity in primary tumors as described in E. All data are presented as mean \pm S.D. (n = 6 independent experiments). ** $P < 0.01$; N.S., not significant. Differences are tested using Mann-Whitney U test.

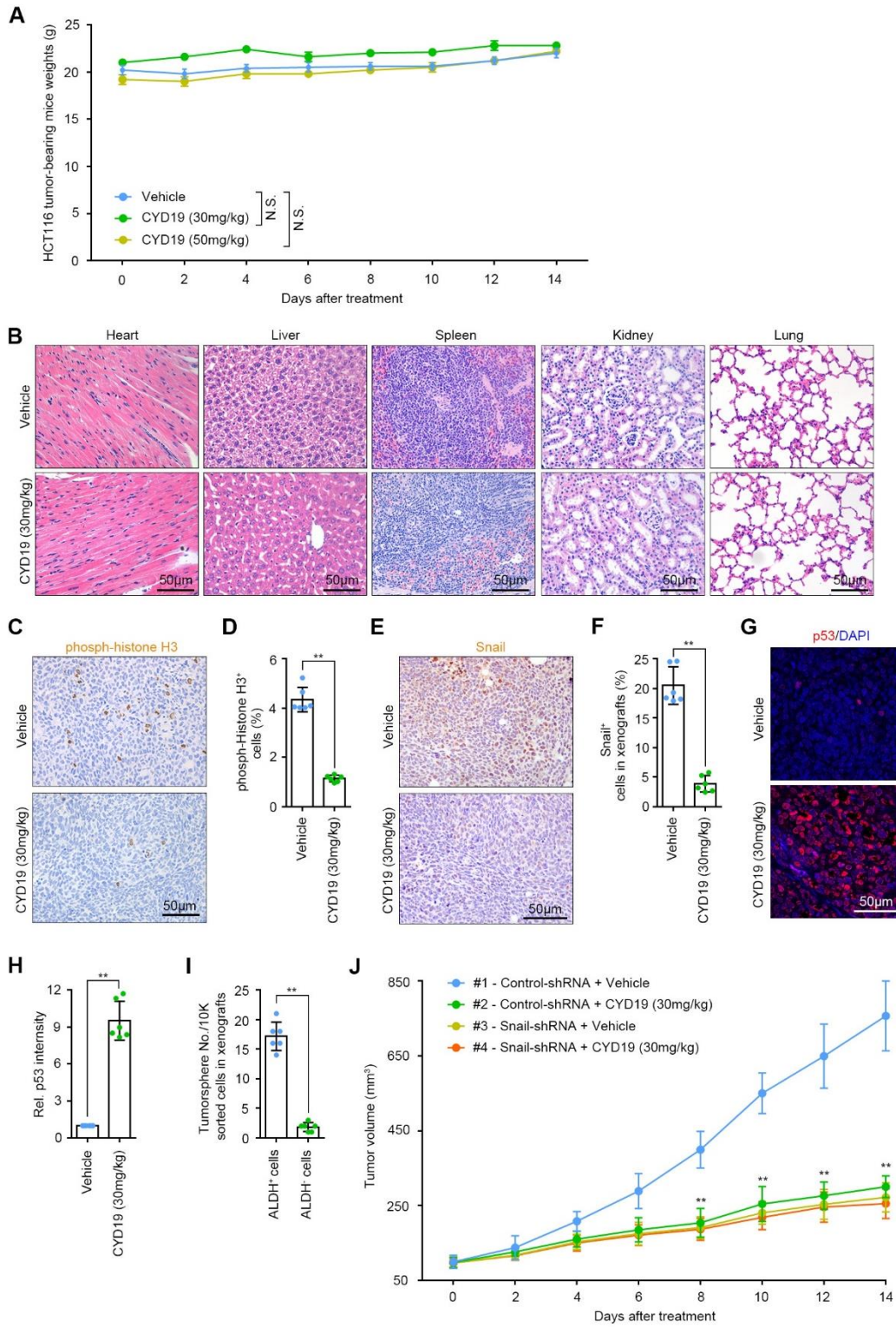


Fig. S7. CYD19 inhibits Snail-driven HCT116 xenograft tumor growth without eliciting toxicity on tumor-bearing mice. (A) Body weights of tumor-bearing mice that were intraperitoneally treated with vehicle or CYD19 for 2 consecutive weeks (n = 6 mice, each). (B) Representative H&E images of key organs of tumor-bearing mice as described in A. (C and E) Immunohistochemical staining of phospho-histone H3 (C) and Snail (E) in xenograft tumors of vehicle- and CYD19-treated mice (n = 6 mice, each). (D and F) Quantification of phospho-histone H3-positive (D) and Snail-positive (F) cells in xenograft tumors as described in C and E, respectively. (G) Immunofluorescence staining of p53 in xenograft tumors as described in C. (H) Quantification of staining intensity in xenograft tumors as described in G. (I) Tumorsphere formation assay of FACS-isolated ALDH⁺ and ALDH⁻ cells from HCT116 xenografts. Equal number of isolated cells (1×10^4 cells) were cultured in ultra-low attachment plates for 1 week, and the tumorspheres were counted. (J) Growth of HCT116 xenograft tumors derived from 1×10^6 control cells or Snail-silenced cells was monitored in nude mice treated with vehicle or CYD19 for 2 consecutive weeks (n = 6 mice, each). All data are presented as mean \pm S.D. (n = 6 independent experiments). ** $P < 0.01$; N.S., not significant. Differences are tested using Mann-Whitney U test.